Supplementary Information

Physical and compositional analysis of differently cultured 3D human skin equivalents by confocal Raman spectroscopy

Y. Dancik,*[a,b] G. Sriram,[a,c,#] B. Rout,[a,b,#] Y. Zou,[a] M. Bigliardi-Qi,[a] P.L. Bigliardi [a,b,d,e]

[a] Experimental Dermatology Laboratory, Institute of Medical Biology, A*STAR, 8a Biomedical Grove, #06-06, Singapore 138648.

[b] Clinical Research Unit for Skin, Allergy and Regeneration, Institute of Medical Biology, A*STAR, 8a Biomedical Grove, #06-06, Singapore 138648.

[c] Faculty of Dentistry, National University of Singapore, 11 Lower Kent Ridge Road, Singapore 119083.

[d] YLL School of Medicine, National University of Singapore & National University Hospital Singapore, 5 Lower Kent Ridge Road, Singapore 119074.

[e] Dept of Dermatology, University of Minnesota, 420 Delaware St SE, Minneapolis, MN 55455, USA.

* Email: yuri.dancik@imb.a-star.edu.sg & pbigliar@umn.edu

[#] Equal authors

Representative full-thickness human skin equivalent histology

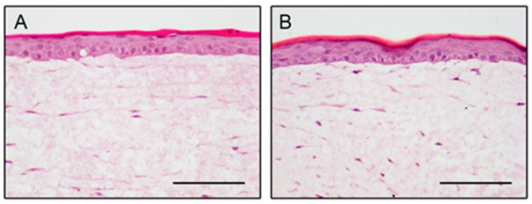

Figure S1 Representative H&E staining of (A) one half of a HSE replicate (16-day airlift culture under normal conditions) used for histology and (B) the other half following full spectroscopic characterisation. Scale bars: 100 μm.

Determination of skin layer thicknesses of full-thickness human skin equivalent samples

For each human skin equivalent (HSE), stratum corneum (SC) and viable epidermis (VE) thicknesses were determined at each location (6 to 7 locations on 3 repeats of each HSE type, see Table 1) at which Raman spectra and a water mass percentage profile were acquired. Thicknesses were then averaged, yielding the mean values and confidence intervals shown in Figure 3C, D and Table 3. The following illustrates the calculation of the thicknesses from the water mass percentage profiles for the first (#1) HSE 16d_IL4-treated.

Locations A and D on HSE 16d_IL4-treated #1 yielded the water mass percentage profiles shown in Figure S2. Also shown are the boundary points and straight lines used to distinguish the SC (P_1 to P_2), VE (P_3 to P_4 and P_5 to P_6) and the dermal matrix (P_7 to P_8). For these and all other water mass profiles used in this study, the boundary points were selected by visually assessing the different regions within the water mass percentage profiles.

Selection of these boundaries was straightforward for most of the profiles across the different HSEs; Fig. S2A is one example. For some profiles, selection of the boundary points defining the SC, VE and dermal matrix was necessarily more subjective, as illustrated in Fig. 2SB. In such cases, regardless of which intersection points for the VE are selected, a linear regression through its regions (lines P_3 to P_4 and P_5 to P_6 in Fig. S2B) yields a relatively poor goodness-of-fit due to the non-linearity in the data. Although the SC-VE and VE-dermal matrix transitions are relatively poorly defined, there was no reason to discard the high wavenumber spectra yielding such water mass percentage profiles. Such discrepancies, even within a single HSE sample, are to be attributed to biological variability. Table S1 below provides the constants for the lines depicted in Fig. S2A and B, defined as Water mass = $m \cdot$ Depth + b, where m denotes each line's slope and b its intercept with the ordinate.

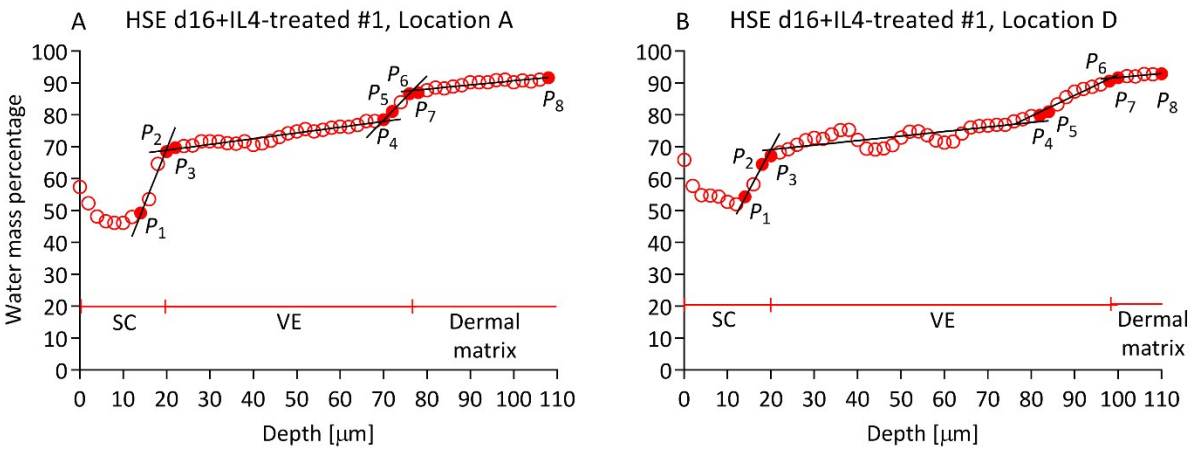

Figure S2 Water mass percentage profiles obtained from HSE 16+IL4-treated #1 at two locations: (A) the first location at which spectra were acquired, termed location A, and (B) the fourth one, termed location D. Measurement points P_1, P_2, etc., are used to define the lines (black) whose intersections yield the depths at which the stratum corneum, the viable epidermis and the dermal matrix intersect. These intersection depths are subsequently used to estimate the thicknesses of the stratum corneum and the viable epidermis.

Table S1 Parameters used to estimate the stratum corneum (SC) and viable epidermis (VE) thicknesses of HSE 16d_IL4-treated #1 at its locations A and D. Refer to Figure S2 for visualization of points P_i and the lines.

		Location A	**Location D**
Depth [μm] of point	P_1	14	14
	P_2	20	18
	P_3	22	20
	P_4	70	82
	P_5	72	84
	P_6	76	98
	P_7	78	100
	P_8	108	110
Line P_1 to P_2	*m*	3.4378	2.5398
	b	0.5838	18.4197
Line P_3 to P_4	*m*	0.1805	0.1417
	b	65.3782	66.3344
Line P_5 to P_6	*m*	1.3930	0.6509
	b	-19.1247	27.6052
Line P_7 to P_8	*m*	0.1303	0.1263
	b	77.7236	79.1900
Thickness [μm]	SC	19.89	19.98
	VE	56.81	78.36

Raman spectroscopy data of human forearm skin and MatTek EpiDermFT™

Figure S3 shows the water mass percentage profiles, as well the stratum corneum ceramide and cholesterol intensity profiles obtained from Raman spectroscopy of *in vivo* human forearm skin and the EpiDermFT™ skin equivalent. For the *in vivo* data, spectra at 9 different locations of a volunteer's left volar forearm were obtained. In the case of EpiDermFT™, spectra at 6 distinct locations on each of 3 skin equivalents from the same batch were acquired.

Following the methodology described above, the stratum corneum thickness obtained from the water mass percentage profiles is (19.7 ± 3.27) μm for the *in vivo* forearm skin and (19.7 ± 3.76) μm for EpiDermFT™. Both values are within the ranges of published *in vivo* values estimated in similar fashion (Table S2). The ceramide and cholesterol intensity profiles shown in Fig. S3 are similar to *in vivo* profiles reported elsewhere[1, 2].

Table S2: Reported volar forearm stratum corneum thicknesses estimated by confocal Raman spectroscopy.

Volar forearm stratum corneum thickness (mean ± SD)	Number of volunteers	Reference
17 ± 2.6 *	15	1
22.6 ± 4.33	14	3
20 ± 3	14	4
19. 5 ± 3.4 (95% CI)	5	5

* Mean of 2 measurements on each of 15 volunteers.

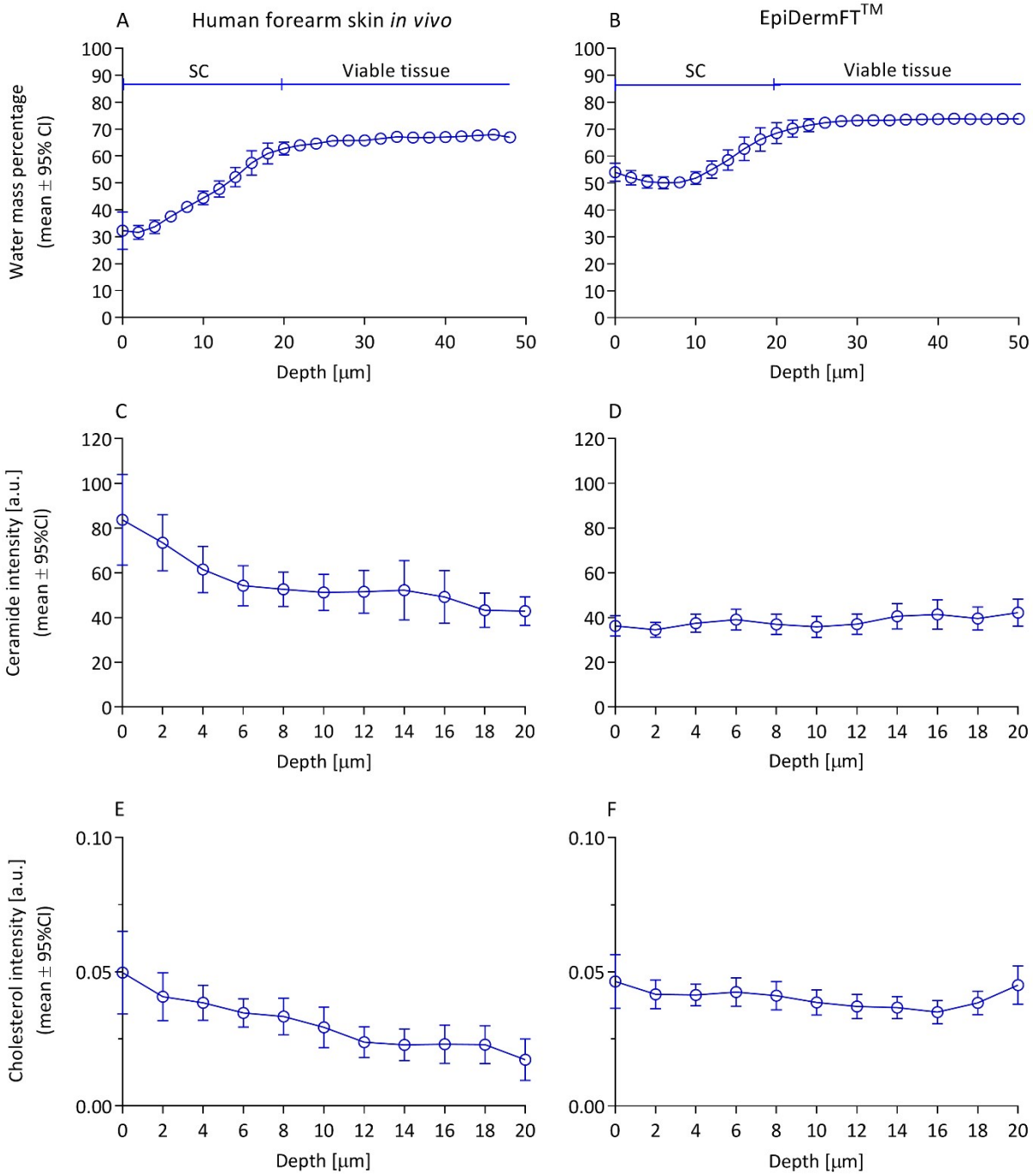

Figure S3 Raman spectroscopic data of human forearm skin and the skin equivalent EpiDermFT™. (A, B) Water mass percentage profiles, (C, D) ceramide intensity and (E, F) cholesterol intensity profiles.

References

1. L. Binder, S. SheikhRezaei, A. Baierl, L. Gruber, M. Wolzt and C. Valenta, *Journal of dermatological science*, 2017, **88**, 280-288.
2. J. Wu and L. Kilpatrick-Liverman, *International journal of cosmetic science*, 2011, **33**, 257-262.
3. M. Egawa, T. Hirao and M. Takahashi, *Acta dermato-venereologica*, 2007, **87**, 4-8.
4. S. Bielfeldt, V. Schoder, U. Ely, A. Van Der Pol, J. De Sterke and K. P. Wilhelm, *International Journal of Cosmetic Science*, 2009, **31**, 479-480.
5. A. Böhling, S. Bielfeldt, A. Himmelmann, M. Keskin and K. P. Wilhelm, *Skin Research and Technology*, 2014, **20**, 50-57.